High gain observed in X-ray induced currents in synthetic single crystal diamonds

A. Lohstroh[*1], **P. J. Sellin**[1], **F. Boroumand**[1], and **J. Morse**[***2]

[1] Department of Physics, University of Surrey, Guildford, GU2 7XH, United Kingdom
[2] European Synchrotron Radiation Facility (ESRF), 6 rue Jules Horowitz, BP 220, 38043 Grenoble, Cedex, France

Received zzz, revised zzz, accepted zzz
Published online zzz

PACS 29.40.Wk, 72.20Jv, 73.40.Rw

Diamond is considered as tissue equivalent, due to its low atomic number, which makes it a particular attractive material for medical radiation dosimetry applications. X-ray dosimeters made of natural single crystal diamonds are commercially available and routinely used, with typical gain values of about 0.5. The selection of suitable natural diamonds for this purpose is time and cost intensive. We report an X-ray induced current study in synthetic single crystal diamonds. Similar to natural diamond dosimeters, the devices had to be pre-irradiated before use to achieve a reproducible performance. We compare two chemical vapour deposited (CVD) samples grown by Element Six Ltd (UK). D1 was a high purity sample contacted in a sandwich structure with an asymmetric contact pair. Sample D2 was cut vertically and contained some nitrogen rich layers. It was contacted with two Ohmic contacts, which partly covered the high temperature/high pressure substrate material. Particle spectroscopy suggests better charge transport in D1 compared to D2, most likely caused by the lower purity. In contrast to this, large gain values up to 6 x 10^4 and a sensitivity of ~30 mC/Gy were measured at field strengths of 2 kV/cm in D2, and only 7 μC/Gy in D1, despite their comparable volumes. We deduce that the gain observed in these devices is affected by the electrical properties of the metal-diamond contacts. The response time of the high gain device was in the order of minutes, which is longer than expected by a purely photoconductive process. Long persistent currents have been reported before in diamond under UV irradiation and modifications of gain and response time by surface treatment of UV detectors are known in the literature, highlighting the influence of the surface and contact interface on the device operation. Our results indicate that synthetic single crystal diamond provides a promising material for high sensitivity tissue-equivalent X-ray dosimeters.

1 Introduction

Diamond is an interesting material for X-ray and ultra violet (UV) light detection, due to its radiation hardness, chemical inertness, large heat conductance, large charge carrier mobilities and low detector dark currents [1, 2]. Its atomic number is considered as tissue equivalent in medical applications, which is particularly beneficial for dosimetry; additionally the spatial resolution of a small solid state detector is far superior to that of a typical gas ionization chamber [3]. Defects in diamond often act as charge trapping centres, degrading the charge transport properties and consequently the detector performance. Natural single crystal diamond X-ray dosimeters have been commercially available for many years but the selection of suitable natural diamonds with the required low defect content for this purpose is time consuming. Grain boundaries act as charge trapping centres in polycrystalline diamond [4], thus high quality single crystalline material is expected to yield larger and more homogenous X-ray induced signals in comparison.

[*] Corresponding author: e-mail: A.Lohstroh@surrey.ac.uk, Phone: +44 1483 689 422, Fax: +44 1483 686 781

 0031-8965/03/0101-0003 $ 17.50+.50/0

We present an initial study of two CVD synthetic single crystal X-ray diamond detectors, concentrating on the induced current signals observed at room temperature, which is one major aspect of the dosimetric application [3]. The current I induced by an incident dose rate D in a detector having a sandwich contact structure is usually described with the formalism for insulating materials introduced by Fowler [5], which assumes Ohmic contact properties. It predicts $I \sim D^{\Delta}$, where Δ is a constant, typically between 0.5 and 1; Δ=1 corresponds to the case where trapping at defect levels limits the carrier life time τ. The photoconductive gain G is defined as the ratio between the current created by the incident irradiation and the current measured in the circuit. According to that model $G = \tau/T_R$ where T_R is the transit time. The electric field in a sandwich structure with the thickness d and an applied bias V is given by V/d. The carrier velocity v can be approximated using the mobility μ, as $v = \mu V/d$, if the velocity is much smaller than the saturation velocity in diamond, which is typically above 8 x 10^6 cm/s [6, 7]. In that case, the transit time is given by $T_R = d^2(\mu V)^{-1}$. Typical values for Δ reported in the literature for single crystal natural and synthetic polycrystalline devices are between 0.8 and 1.1 [8-11]. Natural diamond dosimeters are reported with sensitivities between 50 to 135 $nCGy^{-1}mm^{-1}$ [12]. Polycrystalline X-ray detectors exhibiting gains larger than 1 have been fabricated by several groups [13, 14], and in one instance a gain of 10^6 has been observed in a polycrystalline diamond inter-digitated UV photoconductor [15].

2 Experimental Details

The two diamonds studied here were grown by Element Six Ltd.(UK) using microwave CVD processes. The high purity sample D1 contained a square Ni/Pd/Au top contact with a thinner 0.8 mm diameter area in the centre of the pad [16]. On the back, an Ohmic metal carbide contact had been fabricated [17]. Sample D2 had metal carbide Ohmic contacts on both surfaces and part of the contact area covered high temperature high pressure synthesized (HTHP) diamond material, which had been used as substrate during the growth; additional nitrogen had been introduced on purpose into a small fraction of the area of the CVD material, where it is concentrated in thin layers parallel to the growth surface. In a cathodoluminescence experiment, these layers have been shown to emit the characteristic nitrogen-vacancy luminescence signature, which is absent outside the layers [18]. Details of the device properties are summarized in table I.

Table 1 Comparison of the device properties of D1 and D2

	D1	D2
Growth process	CVD	CVD and HTHP
Thickness [µm]	350	490
Contact area [mm^2]	4	3.8
Guard ring	Yes – floating	No
Biased contact, irradiated side	Ni/Pd/Au (10 nm/30 nm/130 nm) with 0.8 mm diameter centre of Ni/Au (5 nm/5 nm)	Ti/Au (annealed) (50 nm/300 nm)
Grounded contact, back side	Ti/Pd/Au (annealed) (30 nm/30 nm/130 nm)	Ti/Au (annealed) (50 nm/300 nm)
Dark current up to +/- 150 V	< 3pA	< 3pA
I (V) characteristic under X-ray irradiation	Asymmetric, unstable at negative bias	Symmetric
Response time (fully primed)	~30 s	~3 minutes
Sensitivity at +100 V [μCGy^{-1}]	6.1 to 7.0	29300 +/- 300

The samples were placed at various distances from a broad beam Oxford Instruments (model XTF 5011) X-ray tube with a Mo target operated at 50 kV with anode currents up to 1 mA. The absorbed dose has been estimated using a calibrated ionization chamber in place of the sample, assuming an average ratio

of 3.6 for the mass attenuation coefficients of air and diamond [19], which is correct to within 5 % percent for the energy range of the intensity peak of the bremsstrahlung's spectrum and the characteristic Mo emission lines. Differences due to scattering and absorption at the metallization and the sample/ionization chamber mounting have been neglected. The energy to create an electron hole pair in diamond W_{ehp} was assumed to be 13.2 eV [20], which is in agreement within 3 % of other publications [7, 20, 21] and our own particle induced charge pulse studies, although some recent publications suggested W_{ehp} > 15 eV [16, 21, 22]. Thus 1 Gys^{-1} corresponds to a created current of 266 $nAmm^{-3}$. The current data was acquired in air using a Keithley 487 picoammeter. The samples were biased through the irradiated contact, which was made of Ni/Pd/Au in the case of D1 and Ti/Au in the case of D2 (see table I).

3 Results and Discussion

The dark current for both samples was below 3 pA in the investigated voltage range. It increased more than linearly above a certain threshold voltage for both bias polarities, which is qualitatively in agreement with the *I(V)* characteristics reported by Rębisz and Pomorski et al. [23, 24]. Figure 1 displays *I(V)* curves under X-ray irradiation. The current of sample D1 is unstable at negative and stable at positive bias. In contrast, the result for sample D2 shows stable and symmetric currents for either bias polarity. Secondly, the amplitude of the photocurrents is three orders of magnitude larger for sample D2 compared to D1.

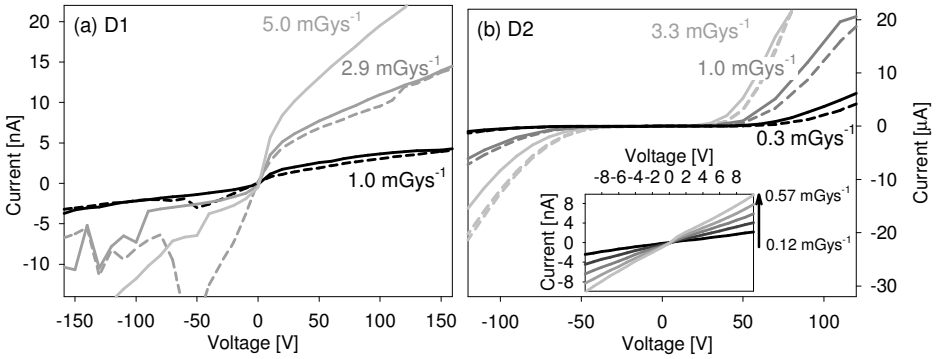

Fig. 1 Current vs voltage under various incident dose rates, solid lines: increasing bias steps, dashed lines, decreasing bias steps. (a) sample D1, (b) sample D2. Inset: induced currents under low bias voltages of sample D2.

Analysis of all the *I(V)* data shows that at a given bias voltage the currents increase linearly with incident dose rate in both detectors (except for the unstable negative bias region of D1). The *I(V)* curves for sample D2 have a small linear region between -10 V and +10 V, displayed in the inset of Fig. 1 (b), where the gain increases linearly with voltage with a rate of about 3.5 V^{-1}, followed by the strong increase in currents at higher biases - and consequently gain up to 6 x 10^4. In contrast the gain shown by device D1 is much smaller and reaches about 18 at +100 V.

The charge transport properties of the diamond material used for both devices have been measured independently in terms of charge collection efficiency (*CCE*) using 2.6 MeV proton induced pulses. The spatially resolved maps of detector response to the proton irradiation showed very low signals in D2 at the layers exhibiting the nitrogen luminescence characteristics, no signal at all was detected from the HPHT substrate [18]. Thus we know that the contribution of these thin layers and the substrate have a negligible contribution to the spectra taken over the whole sample area in Fig. 2 (b).

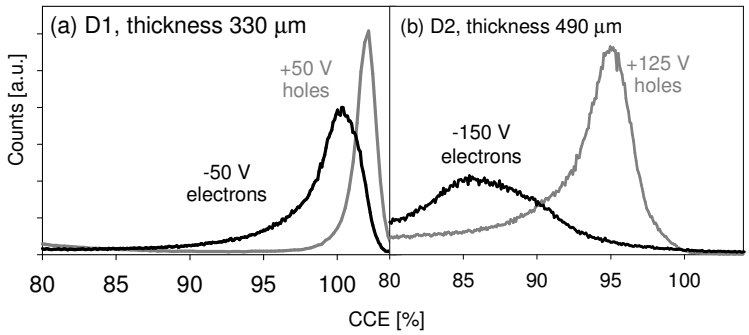

Fig. 2 *CCE* spectra acquired under 2.6 MeV proton irradiation

The *CCE* spectra shown in Fig. 2 demonstrate that D1 has higher and narrower *CCE* peaks at lower applied field strength than D2, which indicates better charge transport properties in this higher purity sample. Therefore we exclude differences in the bulk mobility-lifetime product of the charge carriers as the origin of the much larger induced currents in sample D2. Instead, the different performance is related to the different nature of the metal-diamond contacts, with the gain observed in device D2 due to the symmetric Ohmic carbide contact structure which allows charge injection from the metal contact into the device; this is a requirement for photoconductive gain > 1. In contrast, the top contact in device D1 acts as a (non-ideal) blocking contact which may suppress this injection effect at the metal/diamond interface. This suppression is caused by a potential barrier, which can also depend on dopant concentration. This is expected to be different in D1 and D2 due to their different bulk defect distributions.

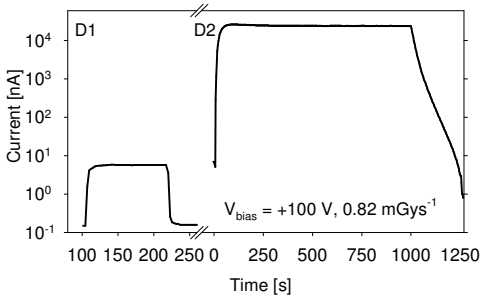

Fig. 3 Time response under switching on and off of the incident X-ray irradiation in the fully primed condition, illustrating the long response times of the devices.

Both samples showed the well-known priming behaviour of diamond during the initial irradiation stage. The signals stabilized after an accumulated dose of ~5 Gy. Figure 3 illustrates that, in the primed state, the time to reach stable current values after a change in incident X-ray dose rate was longer for sample D2 than for D1, with response times of about 3 minutes and 30 s respectively. In both cases, the stabilization takes much longer than it is expected by the simple model of photoconductivity, where the response time is purely limited by the charge carrier life time. Similar persistent photocurrents have been reported in homoepitaxially grown diamond on single crystals [25] and in polycrystalline diamond UV detectors [13], which also showed the trend of slower responses in larger gain devices.

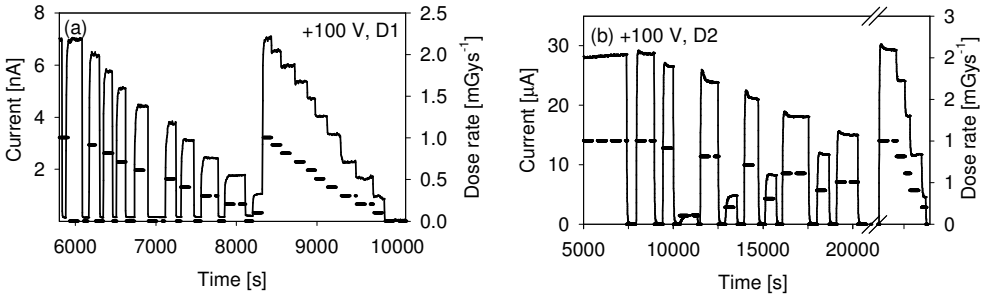

Fig. 4 Induced current (solid) under varying incident dose rates (dashed) in the fully primed state displayed as a function of time (a) sample D1, (b) sample D2.

Figure 4 shows an example of the induced current with varying incident dose rate after priming for each sample. The stabilized photocurrent response is reproducible over timescales of several hours. Datasets such as the one shown in Fig. 4 have been used to extract the sensitivity of each device. The average current at each dose rate has been calculated from the data 30 s after a change in dose rate for D1 and after 3 minutes for sample D2. The results are displayed in Fig. 5. The error bars represent the maximum difference found in each averaged time interval and therefore represent the maximum scatter in the data. The plots indicate an approximately linear current - dose rate relationship ($\Delta \cong 1$), consistent with charge transport affected by traps in both samples in this bias and dose rate regime. The sensitivities found for D1 vary slightly from data set to data set measured under similar conditions, with values between 6.1 and 7.0 µCGy^{-1}. The variation is attributed to a lack of repeatability in the priming procedure, which fails to completely negate the influence of the sample history on the induced currents caused by previous irradiation, illumination and temperature changes. In contrast to that all five extracted sensitivity values of D2 agree within the uncertainty; the mean value is 29.8+/-0.3 mCGy^{-1}, i.e. a gain of ~ 6 x 10^4. Extrapolating from the *I(V)* characteristics, higher gain values are expected at larger bias voltages.

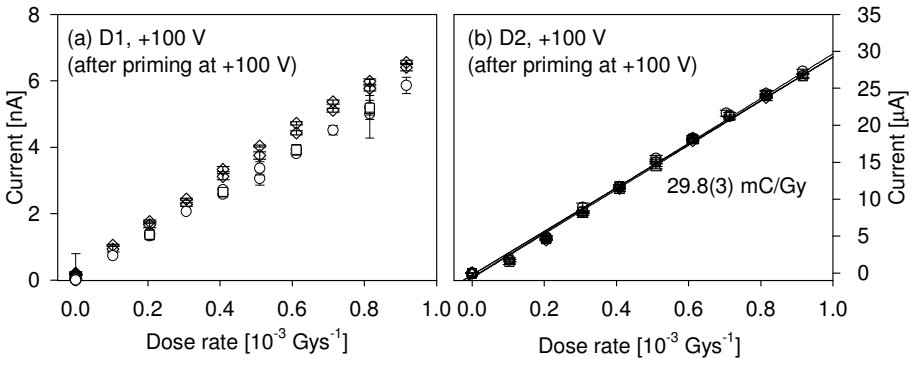

Fig. 5 Sensitivity extracted from data sets exemplified in Fig. 3. (a) sample D1, (b) sample D2. The error bars represent the maximum variation in current values within each averaged interval.

We note that similar high gain values even up to 10^6 have been reported in polycrystalline CVD diamond with a coplanar contact structure under UV illumination by McKeag et al. [15]. In this case, high gain was observed between fine-pitched inter-digitated contacts and was achieved by passivation of near-surface defects in the polycrystalline diamond film.

4 Conclusion

The discrepancy in signal amplitude between radiation induced currents measured in continuous mode compared to induced charge pulses suggests that the result is not purely dependent on the bulk material

quality, but also crucially on the contact characteristics. Further studies using comparable bulk material is needed to clarify the role of the contact processing on the charge injection necessary for the photoconduction process. Nevertheless, our study shows that synthetic single crystal diamond has the potential to be operated as X-ray dosimeter. Despite the high mobility lifetime products observed in single crystal synthetic diamond, a simple model of photoconductive gain cannot explain alone the observed gain of $>10^4$ in our thick 'sandwich' structures. Reproducible gain of the order of 6 x 10^4 has been demonstrated.

Acknowledgements We are grateful to Element Six Ltd. for the supply of their material and for fruitful discussions. We also thank J. Grant, University of Glasgow (UK) for the contact processing of D1 and G. Hill, University of Sheffield (UK) for the contact processing of D2.

References

[1] P. Bergonzo, and R. B. Jackman, in Thin diamond II edited by C. E. Nebel, and J. Ristein, Semiconductors and Semimetals **77**, Elsevier Inc., 2004, Chapter 6, pp. 197-309.
[2] A. Mainwood, Semicon. Sci. Technol. **15**, R55-R63 (2000).
[3] C. Manfredotti, F. Fizzotti, P. Polesollo, E. Vittone, F. Wang, A study of polycrystalline CVD dia mond by nuclear techniques, phys. stat. sol. (a) **154**, 327 (1996).
[4] M. J. Guerrero, D. Tromson, M. Rębisz, C. Mer, B. Bazin, P. Bergonzo, Diamond Relat. Mater.**13** (11-12), 2046 (2004).
[5] J. F. Fowler in Solid state electrical conduction dosimeters, edited by Attix, Roesch, and Tochlin, Radiation Dosimetry **II**, Academic Press Inc. (1966), Chapter 14, p. 308.
[6] H. Pernegger, S. Roe, P. Weilhammer, V. Eremin, H. Frais-Kölbl, E. Griesmayer, H. Kagan, S. Schnetzer, R. Stone, W. Trischuk, D. Twitchen, and A. Whitehead, J. Appl. Phys. **97**, 073704 (2005).
[7] M. Pomorski, E. Berdermann, A. Caragheorgheopol, M. Ciobanu, M. Kiš, A. Martemiyanov, C. Nebel, and P. Moritz for the NoRHDia Collaboration, phys. stat. sol. (a) **203** (12), 3512 (2006).
[8] B. Planskoy, Phys. Med. Biol. **25** (3), 519 (1980).
[9] P. W. Hoban, M. Heydarian, W.A. Beckham, and A. H. Beddoe, Phys. Med. Biol **39,** 1219 (1994).
[10] A. Balducci, Y. Garino, A. Lo Guidice,C. Manfredotti, M. Marinelli, G. Pucella, G. Verona-Rinati, Diamond Relat. Mater. **15**, 797 (2006).
[11] A. J. Whitehead, R. Airey, C. M. Buttar, J. Conway, G. Hill, S. Ramkumar, G. A. Scarsbrook, R. S. Sussmann, and S. Walker, Nucl. Instrum. Methods. A **460**, 20 (2001)
[12] A. Fidanzio, L. Azario, P. Viola, P. Ascarelli, E. Cappelli, G. Conte, and A. Piermattei, Nucl. Instrum. Methods A **524**, 115 (2004).
[13] P. Bergonzo, R. Barrett, O. Hainaut, D. Tromson, C. Mer, B. Guizard, Diamond Relat.Mater. **11**, 418 (2002).
[14] M. Bucciolini, E. Borchi, M. Bruzzi, M. Casati, P. Cirrone, G. Cuttone, C. De Angelis, I. Lovik, S. Onori, L. Raffaele, and S. Sciortino, Nucl. Instrum. Methods. A **552**, 189 (2005).
[15] R. D. McKeag, and R. B. Jackman, Diamond Relat. Mater. **7**, 513 (1998).
[16] J. Morse, M. Salomé, E. Berdermann, M. Pomorski, W. Cunningham, and J. Grant, Diamond Relat. Mater. **16**, 1049 (2007).
[17] M. Werner, Semicond. Sci. Technol. **18**, S41 (2003).
[18] A. Lohstroh, P. J. Sellin, S. G. Wang, A. W. Davies, and J. M. Parkin, Appl. Phys. Lett. **90**, 102111 (2007).
[19] J. H. Hubbell, and S. M. Seltzer, Ionizing Radiation Division, Physics Laboratory National Institute of Standards and Technology, Gaithersburg, MD 20899 (http://physics.nist.gov/PhysRefData/XrayMassCoef/cover.html) (1996).
[20] C. Canali, E. Gatti, F. Kozlov, F. Manfredi, C, Manfredotti, F. Nava, and A. Quirini, Nucl. Instrum. Methods **160**, 73 (1979).
[21] J. Kaneko, and M. Katagiri, Nucl. Instrum. Methods A **383**, 547 (1996).
[22] J. H. Kaneko, T. Kanaka, T. Imai, Y. Tanimura, T. Nishitani, H. Takeuchi, T. Sawaruma, and T. Iida, Nucl. Instrum. Methods A **505**, 187 (2003).
[23] M. Pomorski, E. Berdermann, M. Ciobanu, A. Martemyianov, P. Moritz, M. Rebisz, and B. Marczewska, phys. stat. sol. (a) **202** (11), 2199 (2005).
[24] M. Rębisz, A. Martemiyanov, E. Berdermann, M. Pomorski, B. Marczewska, and B. Voss, Diamond Relat. Mater. **15** (4-8), 822 (2006).
[25] Z. Remes, R. Peterson, K. Haenen, M. Nesladek, and M. D'Olieslaeger, Diamond Relat. Mater. **14**, 556 (2005).